

## Spectroscopic Ellipsometry of Porous n-GaAs

A. Rėza\*, I. Šimkienė, G. J. Babonas, J. Sabataitytė

Semiconductor Physics Institute, A. Goštauto 11, LT-2600 Vilnius, Lithuania

Received 30 September 2003; accepted 21 October 2003

Spectroscopic ellipsometry studies were carried out on porous n-GaAs samples formed by electrochemical etching in HF-based electrolytes. The substrates of n-GaAs:Te ( $n \sim 10^{18} \text{ cm}^{-3}$ ) and n-GaAs:Cr ( $n \sim 10^{14} \text{ cm}^{-3}$ ) were etched in solutions of (1 : 1) HF : H<sub>2</sub>O and (15 : 1 : 1) HF : C<sub>2</sub>H<sub>5</sub>OH : H<sub>2</sub>O, respectively, at various etching times (1 – 30 min) and current densities (30 – 100 mA/cm<sup>2</sup>). The morphology of porous n-GaAs samples was investigated using standard scanning electron microscope (SEM) and atomic force microscope (AFM) techniques. The optical response of porous n-GaAs was studied by means of a photometric ellipsometer in the range 1 – 5 eV. The spectral dependence of experimentally determined ellipsometric parameters was interpreted in the model simulating the complex porous n-GaAs sample as a multilayer structure. A correlation between structural and optical parameters was revealed. The effective parameters obtained in the fitting procedure were used for a characterization of porous n-GaAs samples.

*Keywords:* porous semiconductors, GaAs, spectroscopic ellipsometry, surface morphology.

### INTRODUCTION

The studies of porous semiconductors have been triggered by the discovery of the visible light emission in porous Si (por-Si) [1]. Recently, porous semiconductors other than por-Si have received more interest as the objects of low-dimensional physics as well as new perspective materials for practical applications. In particular, porous III-V compounds were shown to be perspective objects for optoelectronics, non-linear optics and photonics [2].

In the studies of optical properties of porous III-V compounds the main attention was paid to the investigations of luminescence. The samples of porous GaAs (por-GaAs) formed electrochemically possessed luminescence bands in a visible spectral range. On the one hand, in [3] infrared (~840 nm) and visible (~540 nm) luminescence bands were interpreted by quantum confinement effects in micro- and nanocrystallites of GaAs, respectively. On the other hand, in [4] two emission features centered at 548 and 615 nm were assigned to microcrystals of arsenic oxides. In [5] enhanced photoluminescence of por-GaAs was correlated to morphology of the samples and parameters of anodic etching procedure.

Few studies on porous III-V compounds were carried out by spectroscopic ellipsometry technique. From ellipsometric investigations on etched (100) GaSb [6] the thickness, refractive index and dielectric function of residual oxides were estimated. From ellipsometric studies of the optical response of GaSb processed by anodic oxidation [7], the effective refractive index of anodic oxide was determined in two-layer oxide-semiconductor model.

In this work the spectroscopic ellipsometry studies were carried out on a series of n-GaAs substrates etched electrochemically in HF-based electrolytes. It should be emphasized that to our knowledge high resistivity porous n-GaAs has not previously formed and investigated. The main task was to reveal the correlation between particular

features of the optical response and morphology of the samples. The effective parameters, which were obtained from the fitting of experimental spectra by the model calculations, were used for a characterization of complex structure of por-GaAs samples.

### EXPERIMENTAL

The substrates used were n-type Te-doped ( $n \sim 10^{18} \text{ cm}^{-3}$ ) and Cr-doped ( $n \sim 10^{14} \text{ cm}^{-3}$ ) (100)-oriented GaAs wafers. A standard procedure [8] was used to clean the substrate surface. The samples were degreased successively in boiling dimethylformamide, acetone, etched in (3 : 1 : 400) NH<sub>4</sub>OH : H<sub>2</sub>O<sub>2</sub> : H<sub>2</sub>O and rinsed with distilled water. The Au-contact was chemically deposited on the backside of the wafer to achieve uniform etching conditions. The anodic etching procedure on the sample surface area of ~1 cm<sup>2</sup> in size was performed in a teflon cell placed in an ultrasonic bath. The front surface of the sample was illuminated at 600 lx by a standard 100-W incandescent lamp. The wafers of n-GaAs:Te and n-GaAs:Cr were etched in solutions of (1 : 1) HF : H<sub>2</sub>O or HCl : H<sub>2</sub>O and (15 : 1 : 1) HF : C<sub>2</sub>H<sub>5</sub>OH : H<sub>2</sub>O, respectively, for various etching times (1 – 30 min) and current densities (30 – 100 mA/cm<sup>2</sup>). The use of highly concentrated HF-based electrolytes and application of additional illumination has made it possible to form porous structures on high-resistivity n-GaAs.

Standard SEM and AFM techniques were used in the investigations of the surface and cross-section of the por-GaAs structures.

Spectroscopic ellipsometry measurements were performed at 300 K in the range 1 – 5 eV by means of a photometric ellipsometer with rotating analyzer. Systematic errors were taken into account in the on-line data processing procedure. The ellipsometric angles were measured with an accuracy of 0.02°. A total optical response of the sample was characterized by the complex reflection  $\rho$ , which is the ratio between the amplitude reflection coefficients  $R_p$  and  $R_s$  for light polarized parallel ( $p$ ) and perpendicular ( $s$ ) to the plane of light incidence:

\*Corresponding author. Tel.: + 370-5-2619475; fax: + 370-5-2627123.  
E-mail address: [alfa@uj.pfi.lt](mailto:alfa@uj.pfi.lt) (A. Rėza)

$$\rho = \frac{R_p}{R_s} = \tan \Psi \exp(i\Delta), \quad (1)$$

where  $\Psi$  and  $\Delta$  are the ellipsometric parameters. The experimental spectra of  $\Psi(E)$  and  $\Delta(E)$  were fitted by the calculated curves in the model presenting the porous sample as a multilayer structure. The optical response of the stack of layers was calculated by a transfer-matrix technique modeling the propagation of the electromagnetic waves by introducing a 2D vector for electric and magnetic fields and taking into account the boundary conditions at the interface between layers. The final result is presented in the approximation of pseudodielectric function  $\langle \varepsilon \rangle$ , in which the optical response of a complex system is considered [9] as that for isotropic media:

$$\langle \varepsilon \rangle = \sin^2 \Theta \left[ \left( \frac{1-\rho}{1+\rho} \right)^2 \tan^2 \Theta + 1 \right], \quad (2)$$

where  $\Theta$  is the angle of light incidence. In the experiment, the angle  $\Theta = 70^\circ$  was mainly used though some experiments were made at several  $\Theta$ -values.

In the model calculations the reference data for the dielectric function of native oxide [10] and bulk GaAs [11] were used. The porosity of the structural layer was taken into account [12] according to Bruggeman effective medium approximation estimating the volume fraction of material and voids.

## RESULTS AND DISCUSSION

The pseudodielectric function spectra  $\langle \varepsilon \rangle(E)$  for initial n-GaAs:Cr substrate is presented in Fig. 1.

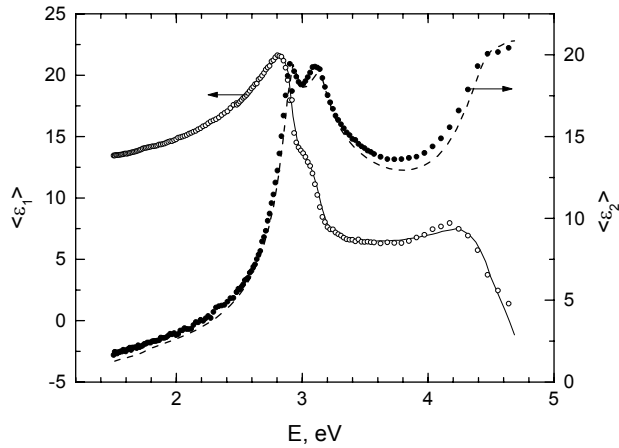


**Fig. 1.** Experimental (points) and calculated (curves) spectral dependence of complex pseudodielectric function of non-etched n-GaAs:Cr

As it is seen from Fig. 1, the experimental  $\langle \varepsilon \rangle$  spectra are well described by model calculations, which include the contribution of surface oxide layer of thickness  $d = 1.7$  nm. Some difference between experimental and calculated data is to be noticed which can be due to neglecting of the non-homogeneity of surface layer in the model.

The  $\langle \varepsilon \rangle(E)$  spectra for n-GaAs:Cr are close to those for bulk crystals [13]. Two main optical features  $E_1$  (at  $\sim 3$  eV) and  $E_2$  (at  $\sim 4.5$  eV) due to interband transitions at

$\Lambda$ - and X-points of the Brillouin zone [13] dominate in the spectra. It should be noted that splitting of  $E_1$  peak due to spin-orbit interaction is well resolved.

The  $\langle \varepsilon \rangle(E)$  spectra for n-GaAs:Te are similar to those presented in Fig. 1 though the optical features  $E_1$  and  $E_2$  are more broadened. From analogues analysis of the  $\langle \varepsilon \rangle(E)$  spectra it followed that the surface oxide layer on n-GaAs:Te substrate was thicker ( $d = 4.8$  nm) and porous (volume fraction of voids  $f_V = 0.39$ ).

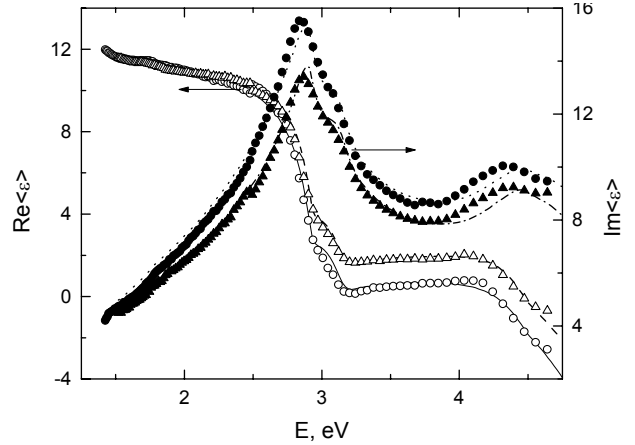


**Fig. 2.** Experimental (points) and calculated (curves) spectra of pseudodielectric function  $\langle \varepsilon \rangle$  of n-GaAs:Te etched for 1 min at 100 mA/cm<sup>2</sup> in (1:1) HCl:H<sub>2</sub>O (circles) and (1:1) HF:H<sub>2</sub>O (triangles)

Figure 2 illustrates the dielectric function of n-GaAs:Te etched for 1 min at 100 mA/cm<sup>2</sup> in electrolytes (1:1) HCl:H<sub>2</sub>O and (1:1) HF:H<sub>2</sub>O. As it follows from comparison of Figs. 1 and 2, the electrochemical etching has led to significant changes of the  $\langle \varepsilon \rangle(E)$  spectra. After etching procedure the absolute values of pseudodielectric function decreased, the spectral changes being considerably stronger in a higher photon energy region.

The modeling of experimental data have shown that the changes in the optical spectra can be explained by the formation of the effective surface layer. The calculated spectra were fitted to experimental data for n-GaAs:Te etched by HCl-based electrolyte with accuracy  $\sim 4\%$  assuming the presence of topmost layer of anodically formed native oxide [10] of thickness 7.0 nm with fractional volume of voids  $f_V = 0.7$  and por-GaAs layer ( $d \sim 10$  nm,  $f_{\text{GaAs}} \sim 0.34$ ). The accuracy was improved to 2.8% assuming that the topmost oxide layer is thicker ( $d \sim 70$  nm) but with a larger porosity ( $f_{\text{GaAs}} \sim 0.009$ ).

Figure 3 shows the SEM image of the n-GaAs:Te etched in (1:1) HCl:H<sub>2</sub>O. As it is seen, the pyramidally-shaped microcrystals up to 10  $\mu\text{m}$  in size were formed at extended surface defects. As follows from previous observations on HCl-etched GaAs [14], the microcrystals observed are predominantly composed of arsenic oxides. In the optical model accepted, the effective layer of anodic native oxide represents the contribution of As<sub>2</sub>O<sub>3</sub> microcrystals to the total optical response.

In the case of n-GaAs:Te etched in HF-based electrolyte, the absolute  $\langle \varepsilon \rangle$ -values (Fig. 2) were higher than those for the samples processed in HCl-based electrolyte. The experimental spectra were described by the model calculations assuming the presence of a non-

homogeneous damaged surface layer of thickness  $\sim 20$  nm with volume fraction  $f_{\text{GaAs}}$  varying in the range 0.1-0.8. This model is in agreement with previous observations on por-n-GaAs:Si ( $1 \times 10^{17} \text{ cm}^{-3}$ ) [15], according which nanometer-scale roughening of the surface can be induced photo-electrochemically by etching in HF-based electrolytes under conditions where no surface passivation takes place. From the structural investigations under SEM it follows (Fig. 4) that the pores/etching pits of 0.2-0.5  $\mu\text{m}$  in size are formed on the sample surface. The contribution of such a rough surface to the optical response is to be compared with that for a damaged/porous layer of GaAs mentioned above. Considering the contribution of porous layer, a structure of stacked multiple layers should be used.

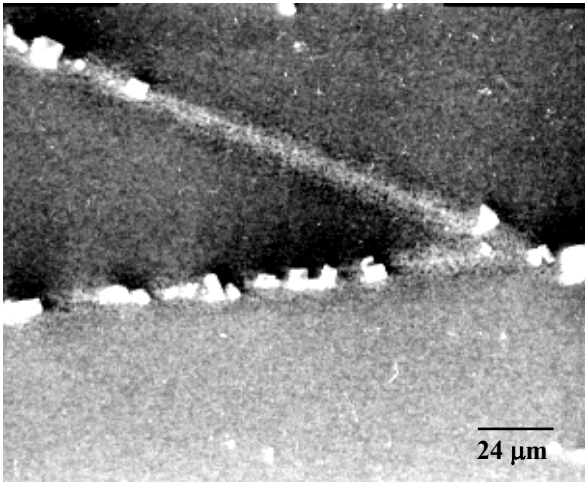


**Fig. 3.** SEM micrograph of the n-GaAs:Te sample etched for 1 min in (1 : 1) HCl : H<sub>2</sub>O at 100 mA/cm<sup>2</sup>

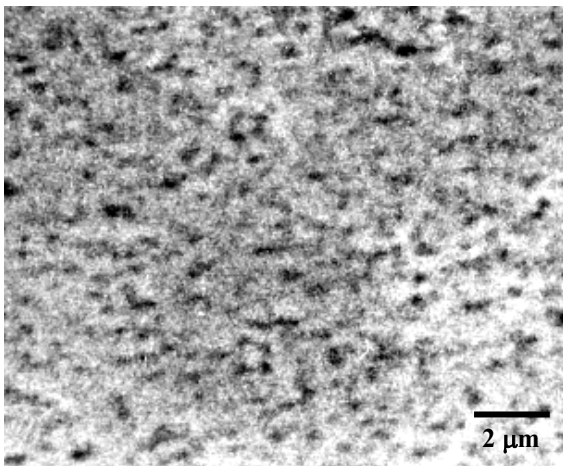


**Fig. 4.** SEM image of the n-GaAs : Te sample etched for 1 min in (1 : 1) HF : H<sub>2</sub>O at 100 mA/cm<sup>2</sup>

Present investigations have shown some particular features in the anodic etching processing of high-resistivity n-GaAs:Cr. At early etching stages, the As<sub>2</sub>O<sub>3</sub> microcrystals of 0.5 – 5.0  $\mu\text{m}$  in size are formed (Fig. 5). The pyramidal-shaped microcrystals are predominantly oriented with respect to the crystallographic axes. At a longer etching time, large ( $\sim 100 - 200 \mu\text{m}$ ) areas free of defects are formed (Fig. 6). These structural features cause the sample non-homogeneity and present significant

difficulties in the characterization of anodically processed high-resistivity n-GaAs : Cr samples by optical technique.

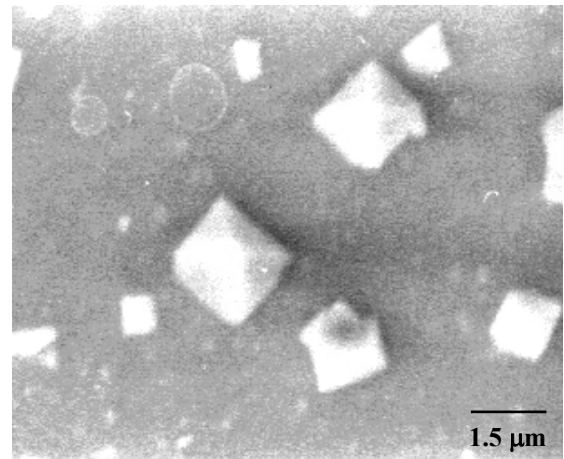


**Fig. 5.** SEM micrograph of n-GaAs : Cr sample etched for 3 min at 30 mA/cm<sup>2</sup> in (15 : 1 : 1) HF : C<sub>2</sub>H<sub>5</sub>OH : H<sub>2</sub>O

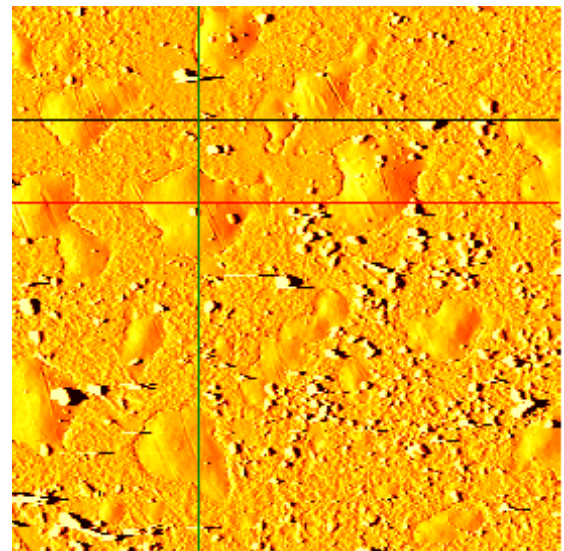


**Fig. 6.** AFM image of surface area 100  $\times$  100  $\mu\text{m}^2$  in the n-GaAs : Cr sample etched for 30 min at 30 mA/cm<sup>2</sup>

The variation of the  $\langle \epsilon \rangle$ -spectra in a series of the n-GaAs:Cr samples etched at 30 mA/cm<sup>2</sup> during various etching time is presented in Fig. 7. As it is seen, even for a short etching time (3 min) the optical features typical of bulk GaAs are significantly distorted indicating the formation of arsenic oxide microcrystals and damaged surface layer on substrate as well as a possible development of oxide layer. In the  $\langle \epsilon \rangle$ -spectra of a long-etched sample ( $t_{etch} = 30$  min) the optical features  $E_1$  and  $E_2$  are completely masked. The absence of interference pattern shows that the surface layers in the etched n-GaAs samples are highly non-uniform and the layer boundaries are non-parallel. An increase of absorption in a higher photon region with the threshold at  $\sim 4.5$  eV indicates a possible formation of Ga<sub>2</sub>O<sub>3</sub> ( $E_g \sim 4.7$  eV [16]) along with As<sub>2</sub>O<sub>3</sub>. It should be noted that the formation of a non-homogeneous surface layer of thickness  $\sim 10 \mu\text{m}$  on anodically processed n-GaAs:Cr (70 mA/cm<sup>2</sup>,  $t_{etch} = 30$  min) was found in photoelectron emission studies [17].

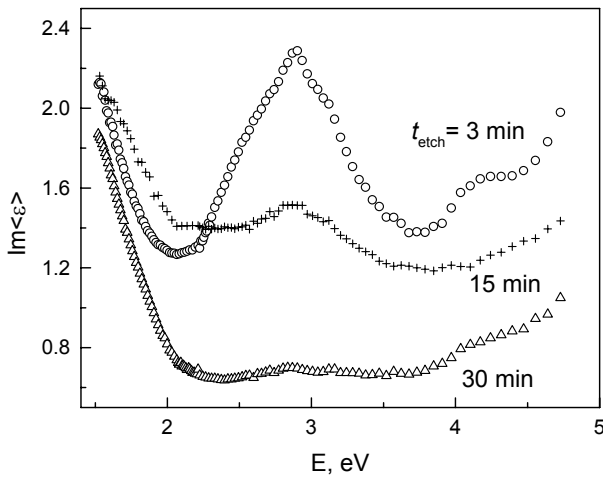


**Fig. 7.** Spectra of  $\text{Im}\langle \epsilon \rangle$  for n-GaAs:Cr etched in various time  $t_{\text{etch}}$  at  $30 \text{ mA/cm}^2$

Figure 8 illustrates the optical response of n-GaAs:Cr sample processed by anodic etching with a surface layer removed chemically by etching in 30% water solution of KOH. As follows from a comparison of Figs. 8 and 1, even for a short etching time ( $t_{\text{etch}} = 3 \text{ min}$ ) the surface of GaAs-substrate is considerably changed. The optical response of this sample (Fig. 8) was well described by the model presenting the structure as the porous top surface layer of native oxide of GaAs of thickness  $\sim 150 \text{ nm}$  and volume fraction  $f_{\text{oxGaAs}} \sim 0.015$ , non-homogeneous oxide layer ( $d \sim 29 \text{ nm}$ ,  $f_{\text{oxGaAs}} = 0.1 - 1.0$ ) and the damaged porous layer of GaAs ( $d \sim 18 \text{ nm}$ ,  $f_{\text{GaAs}} = 0.82$ ). The presence of a native oxide layer can be explained by an active state of GaAs surface after the treatment in KOH water solution.

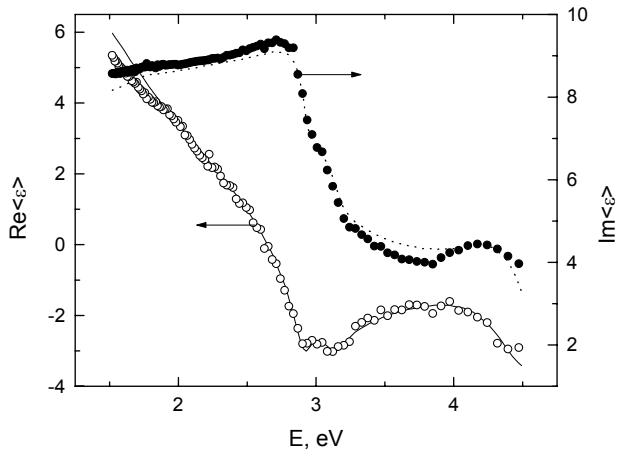


**Fig. 8.** Experimental (points) and calculated (curves)  $\langle \epsilon \rangle$ -spectra of n-GaAs:Cr sample etched for 3 min at  $30 \text{ mA/cm}^2$  with chemically removed surface layer

For a longer times of etching procedure ( $t_{\text{etch}} \sim 30 \text{ min}$ ), the surface oxide layers on n-GaAs substrates are cracked (Fig. 9). The cracks, which are of  $50 - 100 \mu\text{m}$  in size, are oriented along the  $[110]$  direction and indicate the presence of internal strain in the surface layer.

The optical response, which has been obtained from the surface area containing cracks, opens the surface of substrate, which dominates the effective pseudodielectric function (Fig. 10). The experimental data were satisfactorily (7.5%) described by the model of non-

homogeneous ( $d \sim 350 \text{ nm}$ ,  $f_{\text{oxGaAs}} = 0.006 - 0.08$ ) layer of native GaAs oxide and a relatively thick damaged/porous surface layer on substrate ( $d \sim 60 \text{ nm}$ ,  $f_{\text{GaAs}} = 0.3 - 0.7$ ). A significant difference in the structure causes the difference in the optical response of the samples with a dominating contribution of substrate (Figs. 8 and 10). On the basis of these observations it is reasonable to assume that an interface layer between the topmost oxide layer and substrate is formed in anodically processed n-GaAs:Cr samples. In addition, the difference between the real part of  $\langle \epsilon \rangle$  spectra shown in Fig. 1 and 10 is to be noticed which most probably is due to the influence of a scattered light in the cracked surface oxide layer.

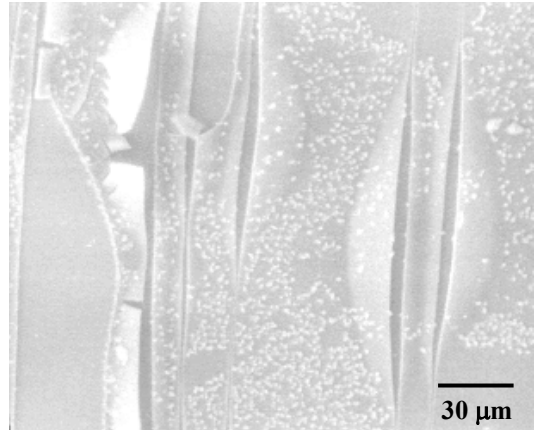


**Fig. 9.** Cracks in the surface layer in SEM micrograph of n-GaAs:Cr sample etched for 30 min at  $30 \text{ mA/cm}^2$

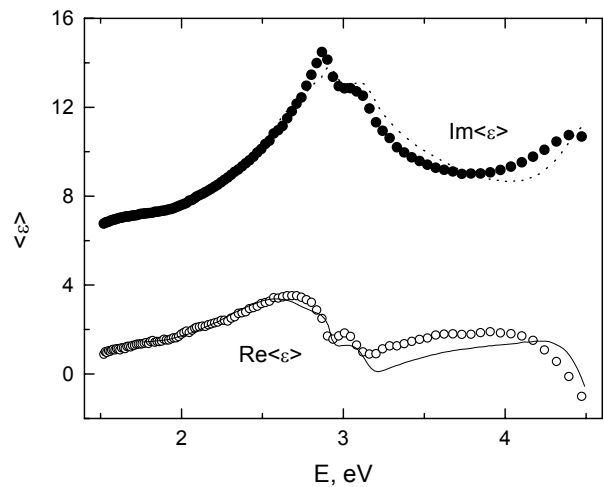


**Fig. 10.** Experimental (points) and calculated (curves)  $\langle \epsilon \rangle$ -spectra of the n-GaAs:Cr samples etched for 30 min at  $30 \text{ mA/cm}^2$  obtained from the surface area with cracks

The structure of the surface layer in the etched n-GaAs:Cr sample is illustrated by Fig. 11. As it is seen from AFM image, the roughness of surface is of order  $40 \text{ nm}$  with grains of  $\sim 200 \text{ nm}$  in size in the sample etched for  $0.5 \text{ min}$  at  $30 \text{ mA/cm}^2$ .

For a longer time of anodic etching procedure, a complete porous surface layer of thickness of order  $\sim 1 \mu\text{m}$  forms (Fig. 12) until it is broken due to internal strains (Fig. 9). In Fig. 12 the  $\text{As}_2\text{O}_3$  microcrystals of  $\sim 10 \mu\text{m}$  in size are seen. The optical response of such structure is

significantly masked because of light scattering. In addition, the modeling of this structure meets some difficulty because of structural non-homogeneity on the surface and in depth.

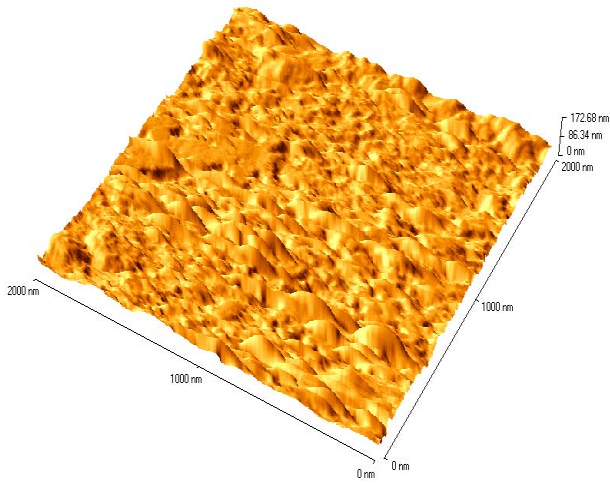


**Fig. 11.** Surface of area  $2 \times 2 \mu\text{m}^2$  of the n-GaAs : Cr sample etched for 30 s at  $30 \text{ mA/cm}^2$

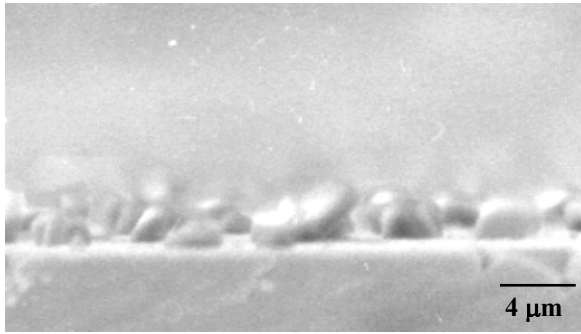


**Fig. 12.** SEM micrograph of the edge of the n-GaAs : Cr sample etched for 30 min at  $30 \text{ mA/cm}^2$

The optical anisotropy of the complex structure formed by anodic processing of the n-GaAs : Cr samples should be noticed. The anisotropy was clearly observed under polarization microscope. The spectral dependence of pseudodielectric function at two orthogonal azimuth orientations of the sample etched for 3 min at  $30 \text{ mA/cm}^2$  is shown in Fig. 13. The in-plane optical anisotropy is illustrated in Fig. 4 as the difference in the pseudodielectric function  $\Delta \langle \epsilon \rangle = \langle \epsilon \rangle_{110} - \langle \epsilon \rangle_{\bar{1}\bar{1}0}$  determined at two orthogonal azimuth orientations of the sample. The anisotropic axes are oriented along the [110] directions

As it is seen from Figs. 13 and 14, the observed optical anisotropy is related to the contribution of GaAs to the optical response. In particular, the spectra of parameters  $\Delta \text{Re} \langle \epsilon \rangle$  and  $\Delta \text{Im} \langle \epsilon \rangle$  (Fig. 14) can be correlated with a simple model of a Lorentzian line the spectral position of which depends on light polarization. In this model in the vicinity of the line, the  $\Delta \text{Im} \langle \epsilon \rangle$  spectrum should possess a dispersion lineshape whereas  $\Delta \text{Re} \langle \epsilon \rangle (E)$  should correspond to the dissipation form. As follows from Fig. 14, the main peak is close to the location of  $E_1, E_1 + \Delta_1$  peaks in bulk GaAs (see Fig. 1). However, as seen from Fig. 13, the lineshape of the spectra for two polarizations do not correspond exactly to the model of the shifted spectral

lines. From the analysis described above, it is evident that the contribution of the oxide layer to the optical response should mask that originated from GaAs.

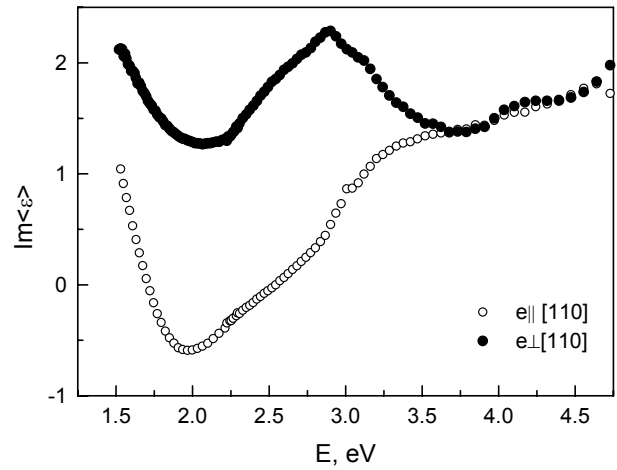


**Fig. 13.** Spectra of imaginary part of the pseudodielectric function measured at two orthogonal orientations of the n-GaAs : Cr sample etched for 3 min at  $30 \text{ mA/cm}^2$

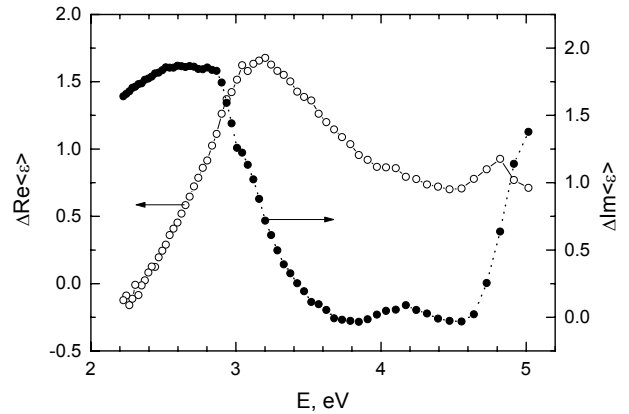


**Fig. 14.** In-plane anisotropy of the pseudodielectric function in the sample n-GaAs : Cr etched for 3 min at  $30 \text{ mA/cm}^2$

As mentioned above, the presence of cracks in the case of thick surface layers indicates large internal stresses. As is known [18], the hydrostatic pressure coefficient for  $E_1$  structure in GaAs is equal to  $7.5 \times 10^{-6} \text{ eV} \cdot \text{cm}^2/\text{kg}$ . Thus, for stresses of order  $\sim 5 \times 10^3 \text{ kg/cm}^2$  the shift of the peaks equal to 10 – 30 meV could be expected. Even for such broadened optical features like these shown in Fig. 13, the shift of this order would cause the optical anisotropy, which is close to that observed experimentally. The optical anisotropy of uniaxially strained GaAs would also originate from the splitting of equivalent  $\Lambda$ -valleys for stress along [111] direction [19].

It should be noted that the optical anisotropy was absent or it was significantly weaker in anodically processed low-resistivity n-GaAs:Te etched at high current densities ( $100 \text{ mA/cm}^2$ ) for a short time (1 min) and in high-resistivity n-GaAs : Cr etched at  $70 - 75 \text{ mA/cm}^2$  for 10 – 30 min.

From the provided structural and optical studies it is possible to propose the following scheme for the anodic etching process in n-GaAs. At early stages of electrochemical etching ( $t_{etch} \sim 0.5 - 3 \text{ min}$ ), the micro-

crystallites of As-oxides, most probably  $\text{As}_2\text{O}_3$ , are formed due to a larger solution rate of As atoms as compared with that of Ga [15]. At a longer etching time ( $t_{\text{etch}} \sim 3 - 5$  min) the size of  $\text{As}_2\text{O}_3$  microcrystallites increases, the presence of significant amount of excess Ga atoms in a solution leads to the formation of Ga-oxides, too. Then, a complete surface layer composed of As- and Ga-oxides begins to form but not as epitaxial one. However, lack of positive charges in high-resistivity n-GaAs:Cr results in a particular action of active fluorine ions leading to the formation of aggregates composed of  $\text{F}^-$  and dipole of GaAs molecules [20]. The clusters of latter aggregates could lead to the formation of GaAs micro-crystals and inclusion them into the surface layer.

## CONCLUSIONS

Summarizing, spectroscopic ellipsometry technique combined with the structural studies is shown to be efficient in the studies of complex structures like anodically processed n-GaAs. The effective parameters, which follow from the fitting of model calculation results to experimental data, can be used for a general characterization of the complex structures.

## Acknowledgment

The work was partially supported by Lithuanian State Science and Studies Foundation (project C-03046).

## REFERENCES

1. **Canham, L. T.** Silicon Quantum Wire Array Fabrication by Electrochemical and Chemical Dissolution of Wafers *Appl. Phys. Lett.* 57 (10) 1990: pp. 1046 – 1048.
2. **Foell, H., Langa, S., Carstensen, J., Christophersen, M., Tiginyanu, I. M.** Pores in III-V Compounds *Advanced Materials* 15 2003: pp. 183 – 198.
3. **Lockwood, D. J., Schmuki, P., Labbe, H. J., Fraser, J. W.** Optical Properties of Porous GaAs *Physica E* 4 1999: pp. 102 – 110.
4. **Finnie, C. M., Li, X., Bohn, P. W.** Production and Evolution of Composition, Morphology, and Luminescence of Microcrystalline Arsenic Oxides Produced During the Anodic Processing of (100) GaAs *J. Appl. Phys.* 86 (9) 1999: pp. 4997 – 5003.
5. **Sabataitytė, J., Šimkienė, I., Bendorius, R.-A., Grigoras, K., Jasutis, V., Pačebutas, V., Tvardauskas, H., Naudzius, K.** Morphology and Strongly Enhanced Photoluminescence of Porous GaAs Layers Made by Anodic Etching *Mater. Sci. Engn. C* 19 2002: pp. 155 – 159.
6. **Papis, E., Kudla, A., Piotrowski, T. T., Golaszewska, K., Kaminska, E., Piotrowska, A.** Ellipsometric Investigations of (100) GaSb Surface Under Chemical Etching and Sulfide Treatment *Mater. Sci. Semicond. Process* 4 2001: pp. 293 – 295.
7. **Sulima, O. V., Bett, A. W., Wagner, J.** Anodic Oxidation of GaSb in Acid-Glycol-Water Electrolytes *J. Electrochem. Soc.* 147 (5) 2000: pp. 1910 – 1914.
8. **Sabataitytė, J., Šimkienė, I., Baranov, A. N., Bendorius, R. A., Pačebutas, V.** Porous  $\text{A}_3\text{B}_5$  Compounds *Mater. Sci. Engn. C* 23 2003: pp. 43 – 48.
9. **Babonas, G. J., Nilisk, A., Reza, A., Matulis, A., Rosental, A.** Spectroscopic Ellipsometry of  $\text{TiO}_2/\text{Si}$  *Proc. SPIE* 5122 2003: pp. 50 – 55.
10. **Aspnes, D. E., Schwartz, B., Studna, A. A., Derick, L., Koszi, L. A.** Optical Properties of Anodically Grown Native Oxides on Some Ga-V Compounds from 1.5 to 6 eV *J. Appl. Phys.* 48 (8) 1977: pp. 3510 – 3513.
11. <http://sopra-sa.com>
12. **Rėza, A., Babonas, G.-J., Rutkūnienė, Ž., Grigonis, A., Galickas, A., Jasutis, V., Kindurys, A.** Optical Response of Ion-Etched Si Structures *Lithuanian J. Phys.* 42 (4) 2002: pp. 285 – 290.
13. **Aspnes, D. E., Studna, A. A.** Dielectric Functions and Optical Parameters of Si, Ge, GaP, GaAs, GaSb, InP, InAs, and InSb from 1.5 to 6.0 eV *Phys. Rev. B* 27 (2) 1983: pp. 985 – 1009.
14. **Li, X., Bohn, P. W.** Arsenic Oxide Microcrystals in Anodically Processed GaAs *J. Electrochem. Soc.* 147 (5) 2000: pp. 1740 – 1746.
15. **Schmuki, P., Fraser, J., Vitus, C. M., Graham, M. J., Isaacs, H. S.** Initiation and Formation of Porous GaAs *J. Electrochem. Soc.* 143 (10) 1996: pp. 3316 – 3322.
16. **Rebien, M., Henrion, W., Hong, M., Mannaerts, J. P., Fleischer, M.** Optical Properties of Gallium Oxide Thin Films *Appl. Phys. Letters* 81 (2) 2002: pp. 250 – 252.
17. **Šimkienė, I., Sabataitytė, J., Karpus, V., Rėza, A., Babonas, G.-J., Čechavičius, B.** Porous Layers on Compensated GaAs:Cr *Mater. Sci. Engn.* (to be published).
18. **Bendorius, R., Šhileika, A.** Electroreflectance Spectra of GaAs at Hydrostatic Pressure *Solid State Commun.* 8 (14) 1970: pp. 1111 – 1113.
19. **Iržikevičius, A., Kavaliauskas, J., Šileika, A.** Au-GaAs Schottky-Barrier Electroreflectance Spectra in the Region of  $E_0$ ,  $E_0+\Delta_0$  and  $E_1$ ,  $E_1+\Delta_1$  Structures Under Uniaxial Stress *Lithuanian J. Phys.* 18 (5) 1978: pp. 57 – 70.
20. **Šimkienė, I.** Semiconductor-Electrolyte Interface in the Technology of Opto-Electronic Devices *Lithuanian J. Phys.* 42 (3) 2002: pp. 231 – 247.

